Available online at www.sciencedirect.com

ScienceDirect

Journal of the European Ceramic Society 30 (2010) 699–704

www.elsevier.com/locate/jeurceramsoc

Low temperature synthesis of tetragonal $BaTiO_3$ by a novel composite-hydroxide-mediated approach and its dielectric properties

Yahong Xie[a,*], Shu Yin[a], Takatoshi Hashimoto[b], Yuichi Tokano[b], Atsushi Sasaki[b], Tsugio Sato[a]

[a] *Institute of Multidisciplinary Research for Advanced Materials (IMRAM), Tohoku University, Sendai 980-8577, Japan*
[b] *NEC Tokin Corporation, Koriyama, Taihaku-ku, Sendai 980-8510, Japan*

Received 15 June 2009; received in revised form 18 August 2009; accepted 27 August 2009
Available online 18 September 2009

Abstract

High purity tetragonal $BaTiO_3$ powders were synthesized by a composite-hydroxide-mediated approach at low temperature using a novel hydrothermal reaction apparatus with a rolling system. The optimum synthesis conditions were explored, and the obtained samples were characterized by their XRD, TEM, TG-DTA and SEM. The powders with an average size of 150 nm in diameter were sintered to almost full theoretical density (ca. 99%) at 1200 °C for 5 h and the obtained ceramics presented a high dielectric constant (9500 at the Curie temperature).

Keywords: $BaTiO_3$; Milling; Sintering; Composites; Dielectric properties

1. Introduction

Barium titanate (BT) has become one of the most important ferroelectric materials used in the electronics ceramic industry. However, conventional synthesis of $BaTiO_3$ involves calcination of a $BaCO_3$ and TiO_2 powder mixture at 1000–1200 °C, and thus often results in polydispersity and the introduction of impurities.[1–5] Numerous studies on developing synthesis methods for purer and finer $BaTiO_3$ powders have been reported in literature.[6–9] Recently, it has been reported that the composite-hydroxide-mediated approach is widely applicable for the synthesis of complex oxide nanostructures. This method is based on a reaction of metallic salts and/or metallic oxides in a potassium hydroxide and sodium hydroxide eutectic melt at around 200 °C in normal atmospheric conditions without using an organic dispersant or capping agent. This methodology provides a one-step, convenient, low-cost, nontoxic, and mass-productive route for the synthesis of nanostructures for functional oxide materials of various structure types.[10,11]

To promote the diffusion of chemical species for a higher reaction rate as well as the uniformity of the product, we chose a novel hydrothermal reaction apparatus with a rolling system (Fig. 1) in this work.[12,13]

2. Experimental

2.1. Synthesis techniques

The $BaTiO_3$ powders were synthesized through a composite-hydroxide-mediated (CHM) approach. A mixture of 40 g of anhydrous hydroxides (NaOH/KOH molar ratio = 51.5:48.5) was put into a Teflon®-lined stainless steel autoclave with 100 cm^3 of internal volume and a 5.5 cm outer diameter, followed by the addition of 30–100 mmol of $BaCl_2$ and TiO_2 (anatase) with 10 Teflon® balls 1.1 cm in diameter. Then, the autoclave was sealed and placed and heated in an electric oven and heated at 200–240 °C for the desired time with a rotation speed of 100 rpm during the reaction. After the reaction, the autoclave was taken out to allow for cooling to room temperature. The product was dispersed in deionized water to remove hydroxide on the surface of the particles, then centrifuged and rinsed with ethanol, deionized water and acetone three times, respectively. Finally, the obtained powders were dried overnight at 60 °C in a vacuum oven.

---

[*] Corresponding author. Tel.: +81 022 217 5599; fax: +81 022 217 5598.
E-mail address: xyh0707@hotmail.com (Y. Xie).

0955-2219/$ – see front matter © 2009 Elsevier Ltd. All rights reserved.
doi:10.1016/j.jeurceramsoc.2009.08.026

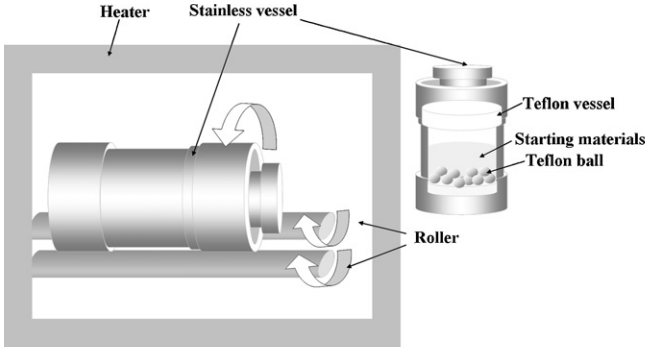

Fig. 1. Schematic diagram of the hydrothermal reaction apparatus with rolling system.

2.2. Characterizations

Thermogravimetric analysis (TG-DTA, Rigaku, TG8101D) was performed for the powders from room temperature to 1200 °C with a heating rate of 10 °C/min in air. The particle morphology was observed by using a transmission electron microscope (JEOL, TEM-2000EX). The X-ray diffraction (XRD) analysis of the obtained powder samples was carried out using CuKα radiation with a pyrolytic graphite monochromator mounted on a powder diffractometer (Shimadzu XD-D1).

The powders were uniaxially pressed at 20 MPa in a steel die to form pellets 20 mm in diameter and 3 mm thick, and then isostatically pressed at 200 MPa. The pellets were then sintered at 1200 °C for 5 h. The morphologies of the sintered bodies were observed by a scanning electron microscope (SEM; Hitachi S-4100). The densities of the sintered pellets were measured by Archimedes' methods. The dielectric constants were determined using an Agilent 4294A precision impedance analyzer.

3. Results and discussion

3.1. Crystalline phase

The explored process parameters of the composite-hydroxide-mediated approach to synthesize the powder of the $BaTiO_3$ were the molar ratio of the starting materials to mineralizer, reaction temperature and reaction time. Fig. 2 shows the XRD patterns of the powders obtained using the composite-hydroxide-mediated approach at 200 °C for 24 h with (a) 30 mmol, (b) 50 mmol, (c) 80 mmol and (d) 100 mmol of $BaCl_2$ and TiO_2 as starting materials and 40 g of anhydrous hydroxides as mineralizer. In the insert, peaks of (0 0 2) and (2 0 0) around $2\theta = 45.5°$ were enlarged to compare the powder tetragonality. All the peaks of the synthesized powders shown in Fig. 2 were consistent with the barium titanate phase with a degree of splitting of the diffraction peak around $2\theta = 45.5°$, which means the high tetragonality, increased with an increase in the molar ratio of the starting materials to mineralizer. It is generally known that the tetragonality diminishes with a decrease in the grain size of $BaTiO_3$. Since all other factors except the amount of starting materials were fixed, it is believed that the increase in tetragonality could be attributed to size differences, i.e., the obtained particle size increased with an increase in the molar ratio of the starting materials to mineralizer.

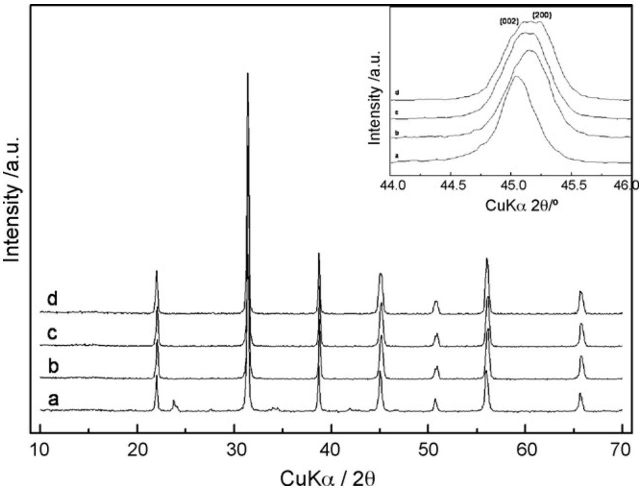

Fig. 2. XRD patterns of $BaTiO_3$ obtained at 200 °C for 24 h with (a) 30 mmol, (b) 50 mmol, (c) 80 mmol and (d) 100 mmol of $BaCl_2$ and TiO_2 as starting materials and 40 g of anhydrous hydroxides as mineralizer.

Fig. 3 shows the dependence of tetragonality on reaction time by the XRD patterns of the powders obtained at 200 °C for (a) 12 h, (b) 24 h, (c) 48 h and (d) 72 h using 50 mmol of $BaCl_2$ and TiO_2 as starting materials. According to the degree of splitting of the diffraction peak at around $2\theta = 45.5°$ shown in the insert, it can be observed that the tetragonality increased with an increase in reaction time.

Fig. 4 is the XRD patterns of (a) commercial $BaTiO_3$ (Sakai, Chemical industry Co., Ltd., BT-05) and prepared $BaTiO_3$ powders at (b) 200 °C and (c) 240 °C for 24 h using 100 mmol of $BaCl_2$ and TiO_2 as starting materials. $BaTiO_3$ particles prepared at 200 °C showed a single peak, but a clear peak splitting could be observed for $BaTiO_3$ particles prepared at 240 °C, which means that the crystal structure of $BaTiO_3$ changed from metastable cubic to tetragonal with an increase in temperature. In contrast,

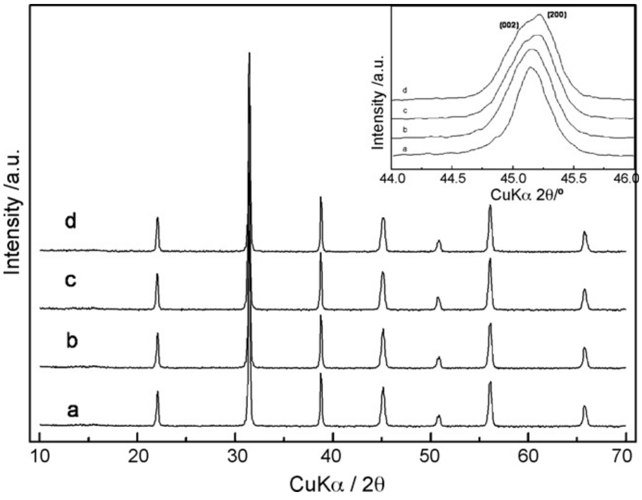

Fig. 3. XRD patterns of $BaTiO_3$ obtained at 200 °C for (a) 12 h, (b) 24 h, (c) 48 h, (d) 72 h using 50 mmol of $BaCl_2$ and TiO_2 as starting material.

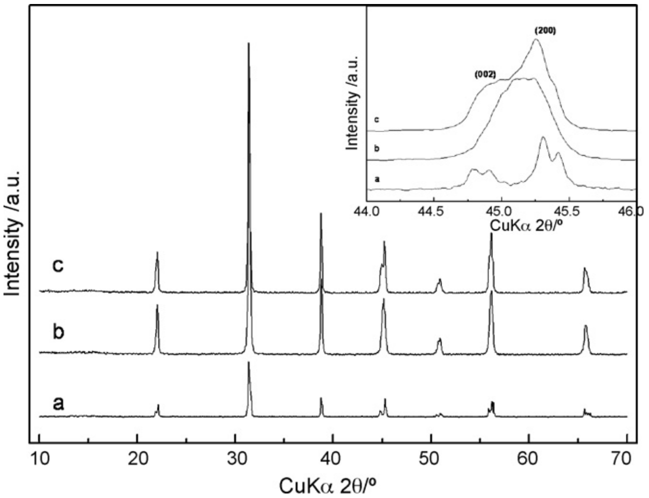

Fig. 4. XRD patterns of $BaTiO_3$ obtained at (b) 200 °C and (c) 240 °C for 24 h with 100 mmol of $BaCl_2$ and TiO_2 as starting material and that of (a) commercial $BaTiO_3$.

the commercial $BaTiO_3$ showed a higher tetragonality probably because of the larger crystallite size.

3.2. Morphology

Fig. 5 shows the TEM images for $BaTiO_3$ prepared using the composite-hydroxide-mediated approach. Fig. 5(a–d) exhibits the dependence of morphology of the powders on the amount of starting materials. The average particle sizes increased from 50, 90, 130 to 150 nm with an increase in the amounts of starting materials from 30, 50, 80 to 100 mmol, respectively. The shapes of the obtained $BaTiO_3$ particles were of cubes, and varied slightly with increases in the amount of starting materials. Fig. 5(e–h) shows the dependence of morphology of the obtained particles on reaction time. The average particle size of $BaTiO_3$ obtained at 200 °C using 50 mmol of $BaCl_2$ and TiO_2 increased with time as 80 nm (12 h), 90 nm (24 h), 200 nm (48 h) to 200 nm (72 h) and the shape tended to change from a cube to

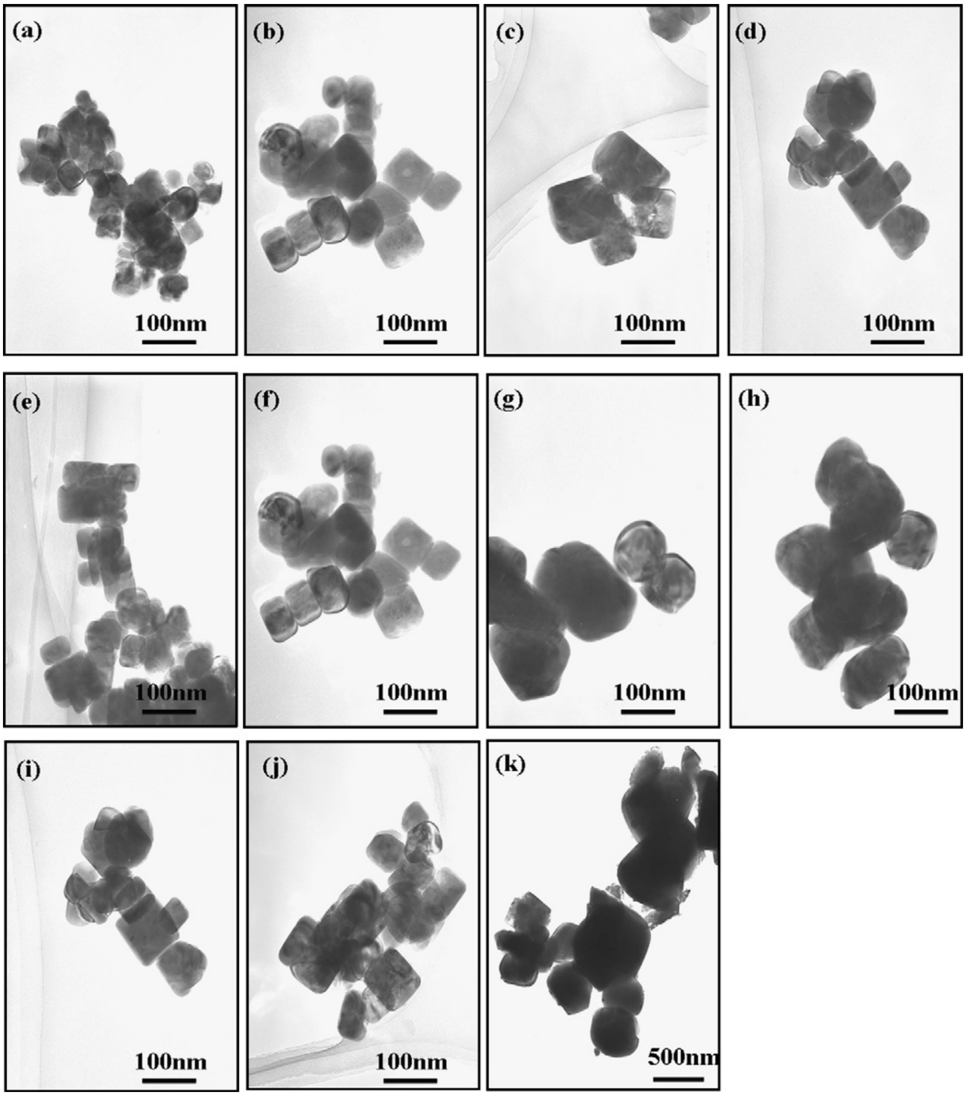

Fig. 5. TEM images of $BaTiO_3$ obtained at 200 °C for 24 h with (a) 30 mmol, (b) 50 mmol, (c) 80 mmol and (d) 100 mmol of $BaCl_2$ and TiO_2 as starting materials, at 200 °C for (e) 12 h, (f) 24 h, (g) 48 h and (h) 72 h using 50 mmol of $BaCl_2$ and TiO_2 as starting material, and at (i) 200 °C and (j) 240 °C for 24 h using 100 mmol of $BaCl_2$ and TiO_2 as starting material and (k) commercial $BaTiO_3$.

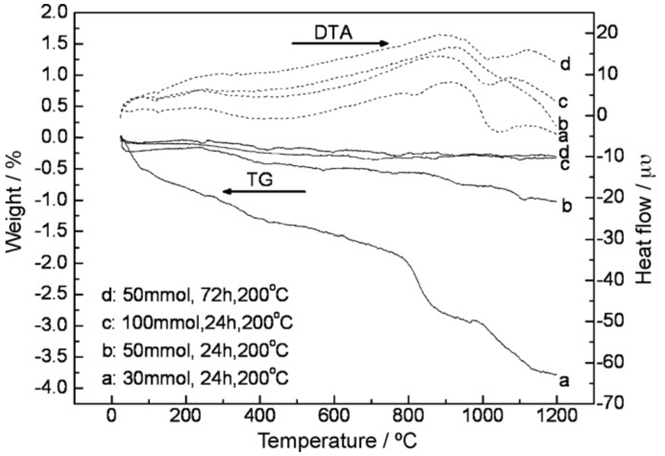

Fig. 6. TG-DTA curves of the samples obtained at 200 °C for 24 h using (a) 30 mmol, (b) 50 mmol and (c) 100 mmol of $BaCl_2$ and TiO_2 as starting materials, and (d) for 72 h using the 50 mmol of $BaCl_2$ and TiO_2 as starting materials.

a sphere. $BaTiO_3$ obtained at 200 and 240 °C using 100 mmol of $BaCl_2$ and TiO_2 as starting materials consisted of cubes of a similar diameter of ca. 150 nm (Fig. 5(i and j)) which was much smaller than that of the commercial one at 400–600 nm (Fig. 5(k)), indicating that when compared with the commercial $BaTiO_3$ particles, $BaTiO_3$ prepared in the present study exhibited a smaller particle size (50–150 nm) in a greater quantity and with a regular cubical shape.

3.3. Thermal analysis

The TG-DTA curves of the samples obtained at 200 °C for 24 h using (a) 30, (b) 50 and (c) 100 mmol of $BaCl_2$ and TiO_2 as starting materials, and (d) for 72 h using 50 mmol of $BaCl_2$ and TiO_2 as starting materials are shown in Fig. 6. The samples showed three steps of weight loss. The weight loss up to 200 °C, 200–800 °C and above 800 °C may be due to the elimination of water adsorbed on the surface, dehydration from the OH^- incorporated in the lattice and elimination of CO_2 from the contaminated $BaCO_3$, respectively. The samples (a) showed a relatively large weight loss such as ca. 2% in the temperature range of 200–800 °C and 1.8% above 800 °C, probably due to poor crystallinity of the sample. The weight loss could greatly be decreased by increasing the amount of starting material and reaction time. It is notable that the whole weight loss of samples (c) and (d) were less than 0.3%, indicating formation of high purity stoichiometric $BaTiO_3$ powder.

$BaTiO_3$ particles should have a tetragonal rather than a cubic structure to achieve a high dielectric constant. In the following context, the sinterability and dielectric properties of the $BaTiO_3$ samples with higher tetragonality obtained at 200 and 240 °C for 24 h using 100 mmol of $BaCl_2$ and TiO_2 as starting materials will be discussed.

3.4. Sinterability

The sample powder obtained at 200 °C for 24 h using 100 mmol of $BaCl_2$ and TiO_2 as starting materials was sintered at various temperatures for 5 h with a heating rate of 10 °C/min. Fig. 7 shows the densities of the sintered bodies as a function of the sintering temperature. The samples could be sintered to a 95.6% theoretical density at a low temperature of 1050 °C, while it could reach 99.1% at 1200 °C, which is much higher than the relative density of 90.3% (5.39 g cm^{-3}) for the sintered body of commercial $BaTiO_3$ at 1200 °C.

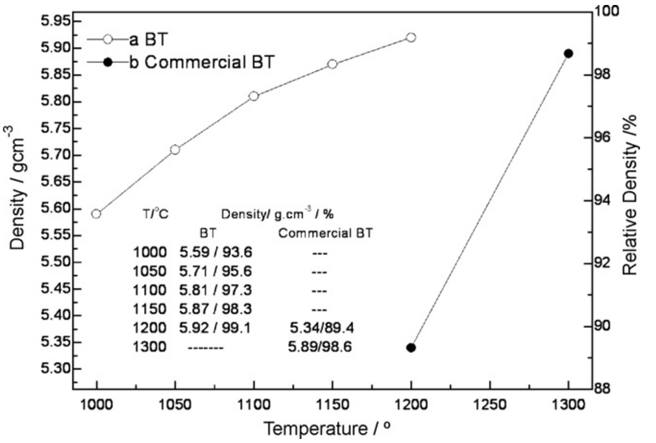

Fig. 7. Temperature dependence of the density of the samples sintered using (a) prepared $BaTiO_3$ and (b) commercial $BaTiO_3$.

3.5. Phase and morphology of ceramics body

$BaTiO_3$ powders prepared using 100 mmol of starting materials at 200 and 240 °C for 24 h were sintered at 1100 and 1200 °C for 5 h. The densities of the samples are listed in Table 1 together with those of commercial $BaTiO_3$ sintered at 1200 °C for 5 h.

Fig. 8 shows the XRD patterns of the sintered bodies of $BaTiO_3$. All peaks could be attributed to the perovskite type $BaTiO_3$ and no other impurity phase could be detected. From Fig. 8, it is clear that the degree of splitting of the diffraction peak at $2\theta = 45.5°$ was enhanced with an increase in the sintering temperature from 1100 to 1200 °C, and in addition, the crystal structure of $BaTiO_3$ was changed from metastable cubic to tetragonal. The samples prepared from the powders obtained at 240 °C showed the higher tetragonality than those obtained at 200 °C. All samples prepared in the present study exhibited higher tetragonality than the commercial $BaTiO_3$ after sintering.

Fig. 9 shows the fracture surfaces of the sintered $BaTiO_3$. It can be observed that the fracture surfaces are irregular and

Table 1
Densities of the samples sintered at 1100 and 1200 °C using the powders prepared at 200 and 240 °C for 24 h with 100 mmol TiO_2 and $BaCl_2$ together with that of commercial powder.

Sample	Powder preparation temperature (°C)	Sintering temperature (°C)	Density (g cm^{-3})/%
	240	1100	5.85/97.3
	240	1200	5.93/99.3
	200	1200	5.92/99.1
	Commercial powder	1200	5.39/90.3

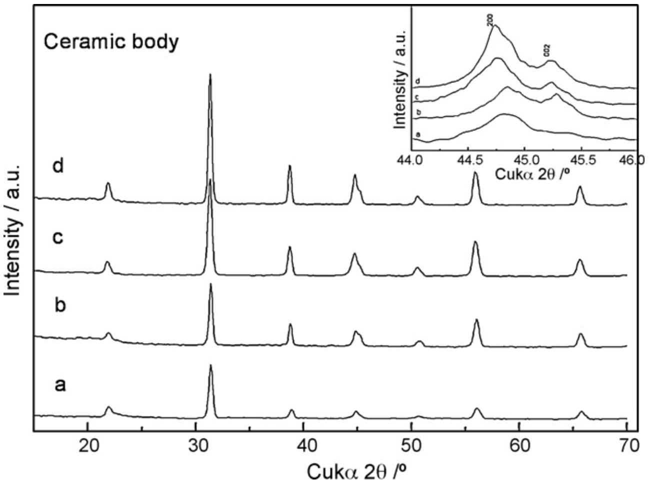

Fig. 8. XRD patterns of ceramic bodies. (a) Commercial $BaTiO_3$ sintered at 1200 °C for 5 h, (b) samples obtained at 240 °C for 24 h and sintered at 1100 °C for 5 h, (c) samples obtained at 200 °C and (d) 240 °C for 24 h using 100 mmol of $BaCl_2$ and TiO_2 as starting materials and sintered at 1200 °C for 5 h.

the grain size was significantly increased from 1 to 10 μm with an increase in sintering temperature from 1100 to 1200 °C. For the samples sintered at 1200 °C, the grain size and morphology showed a little difference, even though the powders were prepared at different temperatures. Comparing the sintered body with the commercial $BaTiO_3$ powder, the specimens sintered using present $BaTiO_3$ powders showed a smaller grain size.

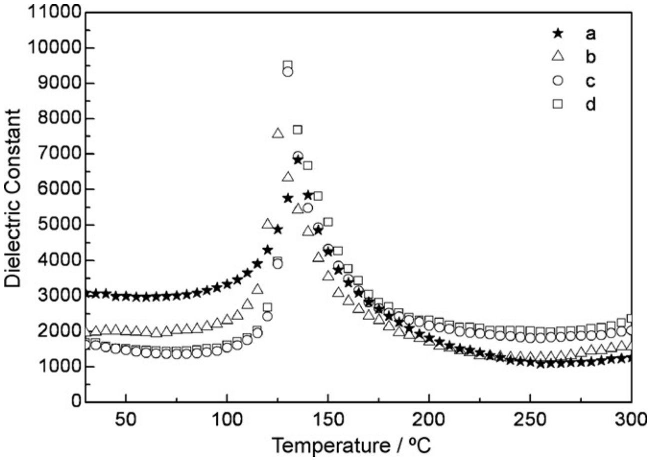

Fig. 10. Dielectric properties of the samples. (a) Commercial $BaTiO_3$ sintered at 1200 °C for 5 h, (b) samples obtained at 240 °C for 24 h and sintered at 1100 °C for 5 h, (c) samples obtained at 200 °C and (d) 240 °C for 24 h using 100 mmol of $BaCl_2$ and TiO_2 as starting materials and sintered at 1200 °C for 5 h.

3.6. Dielectric properties of sintering body

Temperature dependence of the dielectric constant of $BaTiO_3$ measured in air at a frequency of 1 kHz is depicted in Fig. 10. The profiles of the samples sintered at 1200 °C using the powders prepared at 200 and 240 °C were almost identical, showing a maximum value of 9500 at the Curie temperature of ca. 130 °C. In contrast, the sample sintered at 1100 °C showed a lower

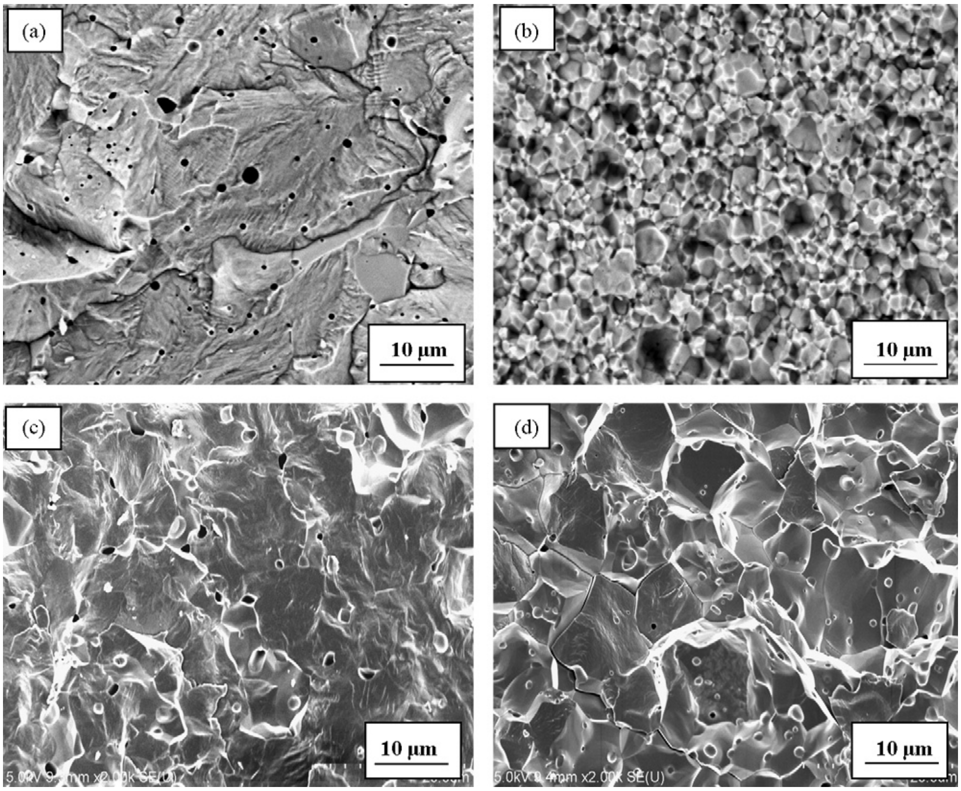

Fig. 9. SEM images of the fracture surfaces of sintered bodies. (a) Commercial $BaTiO_3$ sintered at 1200 °C for 5 h, (b) samples obtained at 240 °C for 24 h and sintered at 1100 °C for 5 h, (c) samples obtained at 200 °C and (d) 240 °C for 24 h using 100 mmol of $BaCl_2$ and TiO_2 as starting materials and sintered at 1200 °C for 5 h.

dielectric constant at the Curie temperature, yet a higher value at room temperature.

In comparison with our synthesized samples, the commercial $BaTiO_3$ showed a higher dielectric value of ca. 3000 at room temperature, but lower dielectric constant value of ca. 6800 at the Curie temperature, which is resulted from the larger grain size and lower density.

4. Conclusions

High purity tetragonal $BaTiO_3$ powders were synthesized by a composite-hydroxide-mediated approach with a novel hydrothermal reaction apparatus with rolling system at 200–240 °C. The powders with average diameter of 150 nm were sintered to nearly full theoretical density at much lower sintering temperature of 1200 °C for 5 h than that of commercial powder. The obtained ceramics presented high dielectric constant (9500) at the Curie temperature. This work provides a one-step, convenient, low-cost, nontoxic, and mass-production route for the synthesis of high purity tetragonal $BaTiO_3$.

Acknowledgements

This research was partially supported by the Ministry of Education, Culture, Sports, Science and Technology, “Special Education and Research Expenses, Post-Silicon Materials and Devices Research Alliance” and the G-COE program “International Center of Research & Education for Molecular Complex Chemistry (IREMC)”.

References

1. Polla, D. L. and Lorraine, F. F., Processing and characterization of piezoelectric materials and integration into microelectromechanical systems. *Chemistry of Materials Annual Review of Materials Science*, 1998, **28**, 563.
2. Takenaka, T. and Nagata, H., Current status and prospects of lead-free piezoelectric ceramics. *Journal of the European Ceramic Society*, 2005, **25**, 2693.
3. McCormick, M. A. and Slamovich, E. B., Microstructure development and dielectric properties of hydrothermal $BaTiO_3$ thin films. *Journal of the European Ceramic Society*, 2003, **23**, 2143.
4. Xinhua, Z., Jianmin, Z., Shunhua, Z., Zhiguo, L., Naiben, M. and Dietrich, H., $BaTiO_3$ nanocrystals: hydrothermal synthesis and structural characterization. *Journal of Crystal Growth*, 2005, **283**, 553.
5. Won, H. I., Nersisyan, H. H. and Won, C. W., Low temperature solid-phase synthesis of tetragonal $BaTiO_3$ powders and its characterization. *Materials Letters*, 2007, **61**, 1492.
6. Matsui, K., Noguchi, T., Islam, N. M., Hakuta, Y. and Hayashi, H., Rapid synthesis of $BaTiO_3$ nanoparticles in supercritical water by continuous hydrothermal flow reaction system. *Journal of Crystal Growth*, 2008, **310**, 2584.
7. Mandal, T. K., Characterization of tetragonal $BaTiO_3$ nanopowders prepared with a new soft chemistry route. *Materials Letters*, 2007, **61**, 850.
8. Ma, Y., Vileno, E., Suib, S. L. and Dutta, P. K., Synthesis of tetragonal $BaTiO_3$ by microwave heating and conventional heating. *Chemistry of Materials*, 1997, **9**, 3023.
9. Peng, Z. and Chen, Y., Preparation of $BaTiO_3$ nanoparticles in aqueous solutions. *Microelectronic Engineering*, 2003, **66**, 102.
10. Liu, H., Hu, C. and Wang, Z. L., Composite-hydroxide-mediated approach for the synthesis of nanostructures of complex functional-oxides. *Nano Letters*, 2006, **6**, 1535.
11. Qin, S., Liu, D., Liu, H. and Zuo, Z., Size-dependent selective etching mechanism: cavity formation on barium titanate nanocubes. *The Journal of Physical chemistry C*, 2008, **112**, 17171.
12. Hotta, Y., Tsunekawa, K., Duran, C., Sato, K., Nagaoka, T. and Watari, K., Low-temperature sintering of $BaTiO_3$ powders prepared by a hydrothermal process with ball milling system. *Materials Science and Engineering A*, 2008, **475**, 57.
13. Hotta, Y., Duran, C., Sato, K., Nagaoka, T. and Watari, K., Densification and grain growth in $BaTiO_3$ ceramics fabricated from nanopowders synthesized by ball-milling assisted hydrothermal reaction. *Journal of the European Ceramic Society*, 2008, **28**, 599.